2. I. Findlay, *J. Physiol.* (*London*) **391**, 611 (1987).
3. G. Meissner and J. S. Henderson, *J. Biol. Chem.* **262**, 3065 (1987).
4. H. C. Hartzell and R. E. White, *J. Gen. Physiol.* **94**, 745 (1989); Z. S. Agus, E. Kelepouris, I. Dukes, M. Morad, *Am. J. Physiol.* **256**, C452 (1989).
5. B. Belles, C. O. Malécot, J. Hescheler, W. Trautwein, *Pfluegers Arch.* **411**, 353 (1988).
6. J. Taniguchi, A. Noma, H. Irisawa, *Circ. Res.* **53**, 131 (1983).
7. J. H. Kaplan and G. C. R. Ellis-Davies, *Proc. Natl. Acad. Sci. U.S.A.* **85**, 6571 (1988).
8. J. H. Kaplan, B. Forbush, J. F. Hoffman, *Biochemistry* **17**, 1929 (1978).
9. We monitored $[Ca^{2+}]_i$ with the long-wavelength fluorescent Ca^{2+} indicator fluo-3 [A. Minta, J. P. Y. Kao, R. Y. Tsien, *J. Biol. Chem.* **264**, 8171 (1989)] to minimize photobleaching of the indicator during flash photolysis and to prevent continual degradation of the caged compounds by ultraviolet fluorescence excitation. Enzymatically dissociated guinea pig ventricular myocytes were equilibrated with intracellular solutions through patch-clamp pipettes (1- to 4-megohm tip resistance; 2.5- to 5-megohm series resistance) in the whole-cell configuration. Current recording, flash photolysis, and fluorescence measurement were done as described [P. H. Backx, B. O'Rourke, E. Marban, *Am. J. Hypertension* (*suppl.*) **4**, 416 (1991)]. Caged Ca^{2+} internal solution contained the following: 150 mM *N*-methyl glucamine (NMG), 10 mM Hepes, 1 mM glutathione, 1 mM ATP (sodium salt), 0.1 mM $CaCl_2$, 0.2 mM DM-nitrophen (sodium salt), 10 μM fluo-3 (ammonium salt), and 10 mM butanedione monoxime (pH 7.2 with CH_4O_3S). Caged Mg^{2+} pipette solutions contained 100 mM NMG, 50 mM Hepes, 1 mM glutathione, 10 mM BAPTA (cesium salt), 0.2 to 1 mM MgATP, and 4 to 6 mM DM-nitrophen (sodium salt) (pH 7.2 with CH_4O_3S); fluo-3 was included when $[Ca^{2+}]_i$ was measured. Photolysis-induced changes in $[Mg^{2+}]_i$ and $[MgATP^{2-}]_i$ were estimated with an iterative computer program with the approach of A. Fabiato and F. Fabiato [*J. Physiol.* (*Paris*) **75**, 463 (1979)], assuming 100% lysis after several flashes. For a 0.5 mM MgATP, 4 mM DM-nitrophen internal solution, the flash-induced increases in $[Mg^{2+}]_i$ and $[MgATP^{2-}]_i$ were 0.12 to 47 μM and 0.63 to 111 μM, respectively. External solutions contained 140 mM NaCl, 5 mM CsCl, 10 mM Hepes, 10 mM glucose, 1 mM $MgCl_2$ with Ca^{2+} or Ba^{2+} as the charge carrier where indicated. Na^+ current was inactivated by a 60-ms pulse from the holding potential (−80 to −40 mV) before a test pulse to 0 or +10 mV (test-pulse duration was 20 ms to limit Ca^{2+} entry into the cell). Frequency of stimulation was 0.2 Hz. In some experiments, Na^+ and Cl^- were replaced by NMG and CH_4O_3S, respectively. Unlike cAMP-dependent regulation of I_{Ca} [R. D. Harvey, J. A. Jurevičius, J. R. Hume, *Proc. Natl. Acad. Sci. U.S.A.* **88**, 6946 (1991)], the effects of Mg^{2+} release on I_{Ca} were not influenced by Na^+ removal.
10. C. A. Vandenberg, *Proc. Natl. Acad. Sci. U.S.A.* **84**, 2560 (1987); H. Matsuda, *J. Physiol.* (*London*) **397**, 237 (1988); K. Ishihara, T. Mitsuiye, A. Noma, M. Takano, *ibid.* **419**, 297 (1989).
11. The external solution contained 140 mM NaCl, 5 mM KCl, 1 mM $MgCl_2$, 2 mM $CaCl_2$, 10 mM Hepes, 10 mM glucose, 1 μM tetrodotoxin, 20 μM nitrendipine, and 50 μM glybenclamide (pH 7.4, 10°C). K^+ current records represent current sensitive to removal of external K^+ (largely I_{K1}) [E. Carmeliet, *J. Physiol.* (*London*) **327**, 285 (1982)]. Internal solution contained 80 mM K-glutamate, 20 mM KCl, 10 mM BAPTA (potassium salt), 10 mM Hepes, 1 mM glutathione, 50 μM glybenclamide, 0.2 mM MgATP, and 6 mM DM-nitrophen (sodium salt) (pH 7.2). Holding potential was −40 mV. Estimates of $[Mg^{2+}]_i$ before and after photolysis were calculated as in (*9*).
12. A. M. Gurney, P. Charnet, J. M. Pye, J. Nargeot, *Nature* **341**, 65 (1989).
13. M. Morad, N. W. Davies, J. H. Kaplan, H. D. Lux, *Science* **241**, 842 (1988); D. T. Yue, P. H. Backx, J. P. Imredy, *ibid.* **250**, 1735 (1990).
14. The transient negative phase of the response was also eliminated when higher concentrations of nucleotide were present in the intracellular solution in caged Mg^{2+} experiments. Under these conditions, Mg^{2+} released from DM-nitrophen was entirely bound by the nucleotide, limiting the $[Mg^{2+}]_i$ to less than 1 μM.
15. M. Kameyama, F. Hofmann, W. Trautwein, *Pfluegers Arch.* **405**, 285 (1985).
16. H. C. Hartzell, P. F. Méry, R. Fischmeister, G. Szabo, *Nature* **351**, 573 (1991); R. W. Tsien *et al.*, *J. Mol. Cell. Cardiol.* **18**, 691 (1986); C. R. Artalejo, M. A. Ariano, R. L. Perlman, A. P. Fox, *Nature* **348**, (1990).
17. G. Yount, D. Babcock, W. Ballantyne, D. Ojala, *Biochemistry* **10**, 2484 (1971).
18. A. Fabiato and F. Fabiato, *J. Physiol.* (*London*) **249**, 497 (1975).
19. H.-C. Cheng, S. M. Van Patten, A. J. Smith, D. A. Walsh, *Biochem. J.* **231**, 655 (1985).
20. Protein kinase C activators reportedly stimulate cardiac Ca^{2+} channel activity in single-channel recordings, but have no effect in whole-cell recordings [A. E. Lacerda, D. Rampe, A. M. Brown, *Nature* **335**, 249 (1988)]. Furthermore, the low intracellular Ca^{2+} and Mg^{2+} conditions in our experiments made protein kinase C activation unlikely. As expected, we observed no effect of phorbol 12-myristate 13-acetate (100 nM) on I_{Ca} either in the presence or absence of cytosolic PKC_{19-36} (10 μM) [C. House and B. E. Kemp, *Science* **238**, 1726 (1987)]. In accordance with the lack of demonstrable protein kinase C activity, the inhibitor did not alter the effect of Mg^{2+} release on I_{Ca} (662 ± 214 pA preflash, 1689 ± 434 pA postflash; $n = 4$; $P < 0.05$).
21. P. A. Smith, P. Rorsman, F. M. Ashcroft, *Nature* **342**, 550 (1989).
22. J. I. Goldhaber, J. M. Parker, J. N. Weiss, *J. Physiol.* (*London*) **443**, 371 (1991).
23. H. Irisawa and S. Kokubun, *ibid.* **338**, 321 (1983).
24. A. Yatani *et al.*, *Science* **238**, 1288 (1987).
25. R. T. Tung and Y. Kurachi, *J. Physiol.* (*London*) **437**, 239 (1991).
26. M. P. Anderson *et al.*, *Cell* **67**, 775 (1991).
27. We thank D. T. Yue for comments on the manuscript. Supported by NIH grant HL 36957 (to E.M.) and by training grant HL 07227 (to B.O'R.).

12 February 1992; accepted 13 May 1992

Molecular Localization of an Ion-Binding Site Within the Pore of Mammalian Sodium Channels

Peter H. Backx, David T. Yue, John H. Lawrence, Eduardo Marban, Gordon F. Tomaselli*

Sodium channels are the major proteins that underlie excitability in nerve, heart, and skeletal muscle. Chemical reaction rate theory was used to analyze the blockage of single wild-type and mutant sodium channels by cadmium ions. The affinity of cadmium for the native tetrodotoxin (TTX)-resistant cardiac channel was much higher than its affinity for the TTX-sensitive skeletal muscle isoform of the channel (μI). Mutation of Tyr^{401} to Cys, the corresponding residue in the cardiac sequence, rendered μI highly susceptible to cadmium blockage but resistant to TTX. The binding site was localized approximately 20% of the distance down the electrical field, thus defining the position of a critical residue within the sodium channel pore.

Sodium channels support the flux of millions of Na^+ ions per second while selecting against the many other ions that are present inside and outside cells (*1*). To understand how the pores of Na^+ channels function at the molecular level, one must define which residues line the permeation pathway and how those residues interact with the ions that cross the membrane. Analysis of the protein sequences deduced from cDNAs led to the prediction that Na^+ channels consist of four major symmetrical domains that assemble to form a central pore (*2*, *3*). In K^+ channels, which are encoded as monomers homologous to each of the four Na^+ channel domains (*4*), the loop linking the fifth and sixth transmembrane segments determines ionic selectivity (*5*) and contains the sites that bind K^+ channel–specific drugs and toxins that block the ionic current (*6*). Neutralization of negatively charged amino acids in the analogous segment of the mammalian brain Na^+ channel, known as the SS1-SS2 region, results in decreased sensitivity to TTX and saxitoxin (STX), altered cation selectivity, and decreased single-channel conductance (*7*). Other experiments suggest the presence of overlapping TTX and STX and divalent ion binding sites that are sensitive to modification by sulfhydryl alkylating agents (*8*). To investigate whether the SS1-SS2 region forms the Na^+ channel pore, we first characterized ion permeation for the cardiac and skeletal muscle isoforms of the Na^+ channel. We then mutated a residue in this region that is different in the two isoforms and determined whether it conferred phenotypic idiosyncracies in ion transport and TTX sensitivity.

Both Cd^{2+} and Zn^{2+} block cardiac Na^+ channels much more potently than they block Na^+ channels from nerve or skeletal muscle (*8*, *9*). Cd^{2+} blockage of the μI

P. H. Backx, J. H. Lawrence, E. Marban, G. F. Tomaselli, Department of Medicine, The Johns Hopkins University, Baltimore, MD 21205.
D. T. Yue, Department of Biomedical Engineering, The Johns Hopkins University, Baltimore, MD 21205.
*To whom correspondence should be addressed.

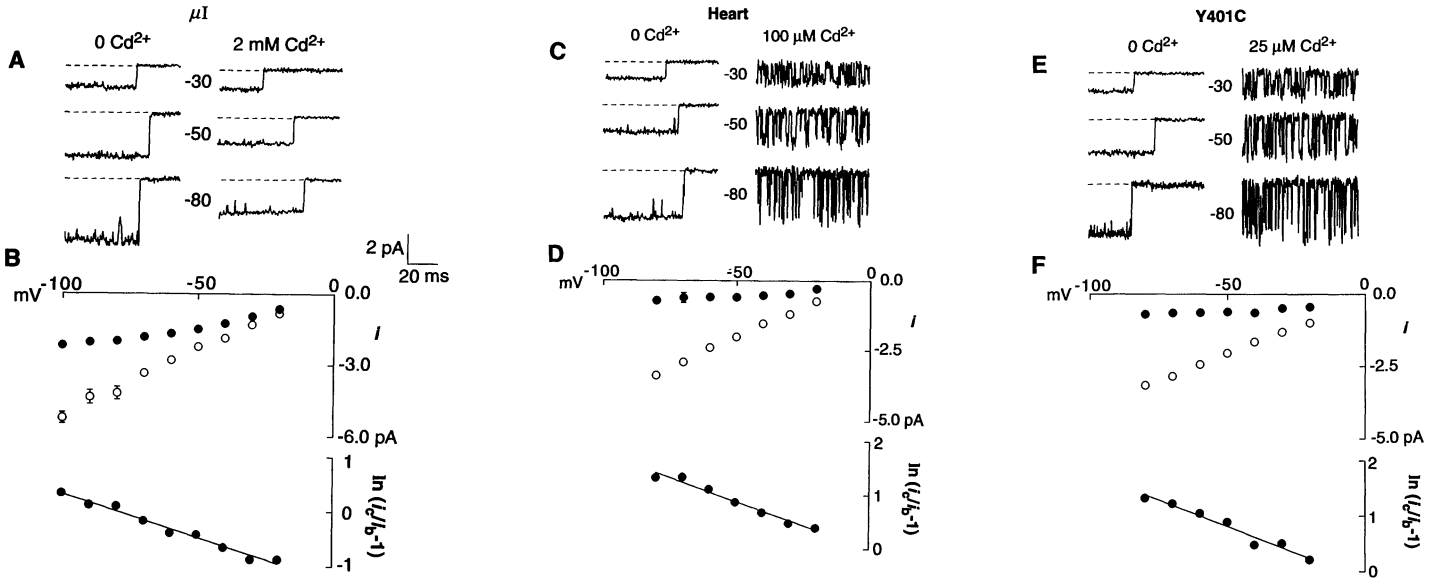

Fig. 1. Cd^{2+} blockage of fenvalerate-modified μI skeletal muscle and cardiac Na^+ channels and the effect of a point mutation. (**A**) Representative single-channel records from oocytes injected with μI RNA in the absence and presence of 2 mM Cd^{2+} at test potentials of −30, −50, and −80 mV. (**B**) (Top) Current-voltage relationships obtained in zero (open circles) and 2 mM (filled circles) Cd^{2+}. The mean ± SE unitary current amplitudes were plotted and the slope conductances were determined by linear regression to the data. (Bottom) A function containing the ratio of the unblocked and blocked current amplitude was plotted against voltage to determine the fractional electrical distance δ (*12*). (**C**) Records from cardiac myocytes in the absence and presence of 100 μM Cd^{2+} at the same potentials shown in (A). (**D**) (Top) The current-voltage relationships of the time-averaged current through cardiac Na^{2+} channels was plotted against voltage in the presence of zero (open circles) or 25 μM (filled circles) Cd^{2+}. Unitary conductances in zero divalents equaled 52 pS (r = .997) for μI (n = 4) and 43 pS (r = .998) for heart (n = 5). (Bottom) A plot as described in (B), bottom, was used to determine δ. (**E**) Single-channel current records from expressed Y401C Na^+ channels exposed to 25 μM Cd^{2+} at test potentials of −30, −50, and −80 mV. (**F**) (Top) The current-voltage relationship of the mutant Na^+ channel variant. Unitary conductance in the absence of Cd^{2+} was 43 pS (r = .998; n = 6). (Bottom) The fractional electrical distance was determined as described in (B), bottom.

skeletal muscle channels expressed in oocytes (*10*) differs significantly from its blockage of native cardiac Na^+ channels (*11*) (Fig. 1, A and C). Single-channel recordings enabled us to distinguish permeation unambiguously from gating during long openings induced by fenvalerate (*10*). With equal concentrations of Na^+ across the membrane and in the absence of divalent cations (Fig. 1, A and C), the two channel types appeared to be very similar, with the μI variant having a slightly larger unitary conductance (Fig. 1, B and D). Nevertheless, the addition of Cd^{2+} to the external solution revealed discrepancies in behavior. Millimolar concentrations of Cd^{2+} reduced unitary current amplitude in the μI channel (Fig. 1A); the reduction in current became more pronounced at increasingly negative potentials. Such behavior is typical of a fast blocker that binds within the pore, with the binding being facilitated by voltage (*1*). The affinity of the blocker for the pore is weak, and the blocking ion occupies the pore so briefly that individual blocking events cannot be resolved; thus, only a reduction in the average current was apparent. The voltage dependence of blockage of the μI channel (Fig. 1B) provides evidence that Cd^{2+} binds somewhere within the electrical field. The fractional electrical distance δ for Cd^{2+} blockage, derived from the ratios of the blocked and unblocked current over a broad voltage range (Fig. 1B), equaled 21%. This value implies that a Cd^{2+} ion entering the channel from the extracellular medium traverses 21% of the full transmembrane field to reach its binding site (*12*).

Comparison of Cd^{2+} blockage of the cardiac channel (Fig. 1C) to its blockage of the μI channel revealed marked differences. First, much less Cd^{2+} (100 μM) was required for blockage of the cardiac channel than for blockage of the μI channel. Secondly, discrete blocking events were evident as brief but complete occlusions of Na^+ flux through the channel. Observation of discrete occlusions of the pore indicates that a Cd^{2+} ion resides longer within the channel and that Cd^{2+} has a higher affinity for its binding site within the cardiac channel relative to the μI channel (*1*, *13*). Comparison of records (Fig. 1C) obtained at different voltages revealed that the channel remains most often in the blocked state at the more negative test potentials. In order to compare directly the potency and voltage dependence of blockage in the two channel types, we calculated the average current through the cardiac channels at each potential (Fig. 1D). The fractional electrical distance δ for Cd^{2+} binding in this case was 22% (*12*) (Fig. 1D). Thus, despite a difference of two orders of magnitude in affinity for Cd^{2+} (*14*), the two channel isoforms bind Cd^{2+} at a virtually identical location within the electrical field (*15*).

The potency of blockage by Cd^{2+} differs so much in the two channel isoforms that it serves as a sensitive marker for subtype-specific pore structure. Nevertheless, the fact that the electrical distance of the Cd^{2+} blockage site is identical in the two isoforms suggests that the distinct binding affinities could arise from a local difference in the structure of the two isoforms. The aligned sequences of the μI and cardiac channels in the SS2 region of the first domain differ at position 401, with Tyr in μI but Cys in the heart clone (*10*, *16*) (Fig. 2A). Cysteine residues have a very high affinity for Cd^{2+} and Zn^{2+} in solution (*17*) as well as in metal-binding proteins such as the Zn^{2+} finger transcription factors (*18*). Sulfhydryl alkylating agents alter the potency of Na^+ channel blockage by Zn^{2+}, which suggests that a Cys side chain contributes to the metal binding site (*8*).

We investigated the importance of residue 401 in μI by constructing a mutant channel in which Tyr was changed to Cys (Y401C) by site-directed mutagenesis (*19*). This mutation reduced the unitary Na^+ channel conductance in the absence of divalent cations from 53 to 43 pS, a value identical to that of the cardiac isoform (Fig. 1E). The mutant channel also behaved like the cardiac isoform when Cd^{2+} was added (Fig. 1E): Cd^{2+} interacted with the pore with high affinity, producing discrete voltage-dependent blockage. The apparent dissociation constant (K_d) for blockage of Y401C by Cd^{2+} was in the micromolar

range, close to the values for the cardiac channel but two orders of magnitude smaller than that for wild-type μI (Fig. 1F). The fractional electrical distance for the site of

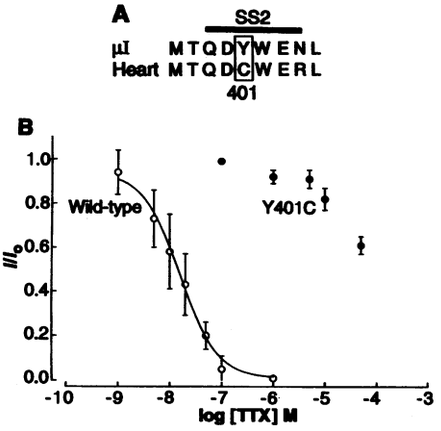

Fig. 2. Effect of a point mutation on blockage by Cd^{2+} and sensitivity to TTX of the expressed μI Na^+ channel. (**A**) The aligned single-letter amino acid sequences of the SS2 region of domain I from the rat μI skeletal muscle (top) (*10*) and rat heart (bottom) (*16*) Na^+ channels, with the numbering scheme based on the μI sequence. The Cys residue in the μI sequence and the corresponding Tyr in the cardiac sequence are highlighted. Abbreviations for the amino acid residues are: C, Cys; D, Asp; E, Glu; L, Leu; M, Met; N, Asn; Q, Gln; R, Arg; T, Thr; W, Trp; and Y, Tyr. (**B**) Normalized whole-cell current measured from a holding voltage of −120 mV to a test potential of −10 mV plotted against TTX concentration for wild-type μI and Y401C (*20*).

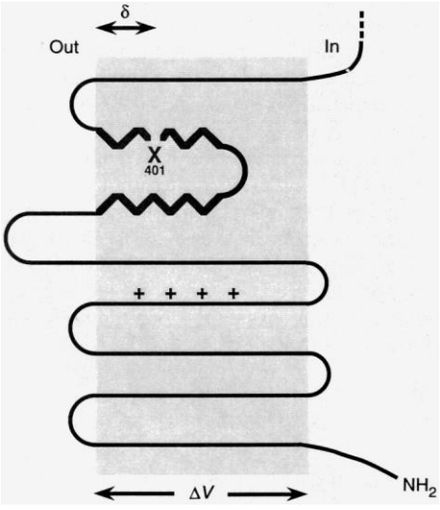

Fig. 3. Model of the transmembrane topology for domain I of the mammalian Na^+ channel based on previous predictions (*3*) and our data. Residue 401 (X) is predicted to lie in the COOH-terminal β sheet at a fractional electrical distance of approximately 0.22 from the extracellular side of the membrane. The shaded region represents the full extent of the transmembrane electrical field.

Cd^{2+} blockage was 24% (Fig. 1F). The fact that the mutant pore conducted Na^+ normally in the absence of divalent cations, coupled with the observation that the location of the Cd^{2+} binding site within the membrane field remained essentially unchanged, indicates that the overall structure of the channel was not radically altered by the Y401C mutation.

The susceptibility of various isoforms of Na^+ channels to blockage by Cd^{2+} and Zn^{2+} varies inversely with sensitivity to blockage by TTX or STX (*9*); indeed, it has been proposed that the toxins and divalents interact with the same binding site (*8*). The cardiac channel is resistant to TTX [median inhibition concentration (IC_{50}) ~3 μM] (*20*); in contrast, the Na^+ current through wild-type μI channels was blocked by nanomolar concentrations of TTX (IC_{50} = 16 ± 2 nM) (Fig. 2B). If TTX and Cd^{2+} share a binding site, the Y401C mutant should exhibit markedly altered TTX affinity. This is indeed the case: micromolar concentrations of TTX are required to inhibit Na^+ current through the mutant channels (IC_{50} > 50 μM) (Fig. 2B) (*21*). Thus, the conversion of a single residue in skeletal muscle μI Na^+ channels alters the sensitivities to blockage by either Cd^{2+} or TTX, producing a phenotype similar to that of the cardiac isoform (*22*). Because TTX is large compared to a Cd^{2+} ion (*1*), it may interact with more than one site when it binds to the channel (*7*). Nevertheless, the fact that TTX can interact so tightly with a residue that is well within the electrical field provides good reason to reexamine the controversial finding that TTX blockage is voltage-dependent (*20*).

The importance of the Cys residue in SS2 is supported by evidence that the reverse mutant, Cys to Tyr in the rat heart Na^+ channel, alters sensitivity to Cd^{2+} and TTX (*23*). These researchers and others have speculated that the site lies outside the field because of evidence that TTX and STX (*23*) or Cd^{2+} (*24*) block in a voltage-independent manner. The voltage dependence of Cd^{2+} blockage in all the channel types we examined places the SS2 segment within the membrane field and further locates the position of a critical residue within the permeation pathway. We propose that the topology of the first domain of the Na^+ channel is similar to that of SS2 in K^+ channels (*3*, *5*, *6*) (Fig. 3). Although others have suggested that the SS1-SS2 loop is extracellular (*2*), our proposed orientation is similar to that based on space-filling models of the primary sequence (*3*).

REFERENCES AND NOTES

1. B. Hille, *Ionic Channels of Excitable Membranes* (Sinauer, Sunderland, MA, ed. 2, 1992).
2. M. Noda *et al.*, *Nature* **312**, 121 (1984).
3. H. R. Guy and P. Seetharamulu, *Proc. Natl. Acad. Sci. U.S.A.* **83**, 508 (1986); H. R. Guy and F. Conti, *Trends Neurosci.* **13**, 201 (1990).
4. E. Y. Isacoff, Y. N. Jan, L. Y. Jan, *Nature* **345**, 530 (1990); W. A. Catterall, *Science* **242**, 50 (1988); C. Miller, *ibid.* **252**, 1092 (1991).
5. A. J. Yool and T. L. Schwartz, *Nature* **349**, 700 (1991); H. A. Hartmann *et al.*, *Science* **251**, 942 (1991).
6. R. MacKinnon and C. Miller, *Science* **245**, 1382 (1989); G. Yellen *et al.*, *ibid.* **251**, 939 (1991); K. L. Choi, R. W. Aldrich, G. Yellen, *Proc. Natl. Acad. Sci. U.S.A.* **88**, 5092 (1991).
7. M. Noda *et al.*, *FEBS Lett.* **259**, 213 (1989); M. Pusch *et al.*, *Eur. Biophys. J.* **20**, 127 (1991); H. Terlau *et al.*, *FEBS Lett.* **293**, 93 (1991); S. H. Heinemann *et al.*, *Nature* **356**, 441 (1992).
8. L. Schild and E. Moczydlowski, *Biophys. J.* **59**, 523 (1991); L. Schild, A. Ravindran, E. Moczydlowski, *J. Gen. Physiol.* **97**, 117 (1991).
9. D. DiFrancesco *et al.*, *Proc. R. Soc. London, Ser. B* **223**, 475 (1985); C. W. Bowers, *Brain Res.* **340**, 143 (1985); C. Frelin *et al.*, *Eur. J. Pharmacol.* **122**, 245 (1986); A. Ravindran *et al.*, *J. Gen. Physiol.* **97**, 89 (1991).
10. An expression plasmid that contained the cDNA encoding the μI channel [J. S. Trimmer *et al.*, *Neuron* **3**, 33 (1989)] was provided by G. Mandel. Complementary RNA was prepared and injected into *Xenopus laevis* oocytes, and membranes were prepared for electrophysiological recording as described [G. F. Tomaselli *et al.*, *Biophys. J.* **60**, 721 (1991)]. Single-channel currents were recorded with an integrating headstage (Axon Instruments, Burlingame, CA), sampled at 10 kHz and low-pass–filtered (4-pole Bessel, −3dB at 2 kHz), and processed as described (*25*). We used the inside-out variant of the patch-clamp technique [O. P. Hamill *et al.*, *Pfluegers Arch.* **391**, 85 (1981)]. Currents were recorded with 140 mM NaCl and 10 mM Hepes (pH 7.4) in the pipette and bath at 23°C; the appropriate concentration of Cd^{2+} or Zn^{2+} was added to the pipette solution. Fast inactivation was blocked by including fenvalerate (2 to 20 μM) in the bath [D. Yamamoto, J. Z. Yeh, T. Narahashi, *Biophys. J.* **45**, 337 (1984); S. F. Halloway, V. L. Salgado, C. H. Wu, T. Narahashi, *Pfluegers Arch.* **414**, 613 (1989)].
11. Guinea pig ventricular cells were prepared by enzymatic dispersion as described (*25*). Currents were recorded as described (*10*).
12. To analyze blockage of wild-type μI Na^+ channels, we assumed a single open state and a single binding site. The probability of being unblocked is given by the ratio of the single-channel current amplitude in the presence of Cd^{2+} (i_b) and that in the absence of divalent cations (i_c). The fractional electrical distance was determined by an adaptation of the method of Woodhull [A. M. Woodhull, *J. Gen. Physiol.* **61**, 687 (1973)] to single-channel records [J. Neyton and C. Miller, *J. Gen. Physiol.* **92**, 549 (1988); R. J. French, J. F. Worley, B. K. Krueger, *Biophys. J.* **45**, 301 (1984)]. The voltage dependence of the probability of being unblocked is described by the equation

$$\ln (i_c/i_b - 1) = \ln ([Cd^{2+}]/K_d) - \delta V\lambda \quad (1)$$

where $\lambda = ze/RT$; R is the gas constant, T is temperature, e is the elementary charge, and z is the valence of the blocking ion. The slope of the plot of the left-hand term of Eq. 1 against voltage is $\delta\lambda$. The value δ is the fractional electrical distance from the extracellular solution to the Cd^{2+} binding site and is determined directly from the slopes of the plots in Fig. 1, B, D, and F (bottom panels). The zero-voltage intercept is the natural logarithm of the ratio of the $[Cd^{2+}]$ and the apparent K_d. The discrete nature of blockage of cardiac and μI Y401C channels allowed explicit determination of the on- and off-rate constants of the Cd^{2+} blocking process and thus the K_d. The voltage dependence of the rate constants provides a measure of the electrical distance associated with Cd^{2+} binding and unbinding. The same assumptions regarding the blocking process were

made as above, and the values for δ and K_d were comparable with the two approaches.
13. P. H. Backx, E. Marban, D. T. Yue, *Biophys. J.* **57**, 298a (1990); S. Visentin *et al.*, *Pfluegers Arch.* **417**, 213 (1990).
14. The K_d's for Cd^{2+} blockage at 0 mV determined from plots of the open probability at various voltages were 6.8 mM for μI (r = 0.995) and 100 μM for native cardiac channels (r = 0.985).
15. In similar experiments, Zn^{2+} blockage of cardiac and μI skeletal muscle Na^+ channels was examined. The K_d's for Zn^{2+} were similar to those measured for Cd^{2+}, and estimates for the electrical distance of the binding site in the membrane field were virtually identical.
16. R. B. Rogart *et al.*, *Proc. Natl. Acad. Sci. U.S.A.* **86**, 8170 (1989).
17. A. E. Martell and R. M. Smith, *Critical Stability Constants: Amino Acids* (Plenum, New York, 1989), vol. 1, p. 47.
18. J. M. Berg, *Annu. Rev. Biophys. Biophys. Chem.* **19**, 405 (1990).
19. The 1.9-kb Bam HI–Sph I fragment from the μ1-2 cDNA (*8*) was subcloned into pGEM-11Zf+ for mutagenesis [T. A. Kunkel, *Proc. Natl. Acad. Sci. U.S.A.* **82**, 488 (1985)]. The entire fragment was sequenced by the dideoxy chain termination method (Sequenase, U.S. Biochemical) [F. Sanger *et al.*, *Proc. Natl. Acad. Sci. U.S.A.* **74**, 5463 (1977)]. In vitro RNA transcription and oocyte injection were done as described (*9*).
20. M. Baer *et al.*, *Nature* **263**, 344 (1976); C. J. Cohen *et al.*, *J. Gen. Physiol.* **78**, 383 (1981); P. M. Vassilev *et al.*, *Am. J. Physiol.* **251**, H475 (1986); B. Hille, *Biophys. J.* **15**, 615 (1975); *J. Gen. Physiol.* **66**, 535 (1975).
21. Oocytes injected with RNA that encoded the wild-type μI Na^+ channel α subunit and the Y401C mutation were voltage-clamped with a two-microelectrode amplifier. Currents were recorded in 96 mM NaCl, 2 mM KCl, 0.5 mM $CaCl_2$, and 5 mM Hepes (pH 7.5). TTX was added to the bath at concentrations from 1 nM to 1 μM (wild type) and 100 nM to 50 μM (Y401C). Peak currents were measured at −10 mV from a holding potential of −120 mV and were normalized to the current in the absence of toxin. The data represent at least three determinations at each concentration from 20 (wild type) and 13 (Y401C) oocytes. The wild-type K_d was determined by a least-squares fit of the data to a logistic function; a similar fit to the Y401C mutant was not possible because of the insensitivity of the variant to TTX (Fig. 2B).
22. The mutant Y401C actually is less sensitive to TTX (K_d > 50 μM) and more sensitive to blockage by Cd^{2+} (K_d at 0 mV = 29 μM; r = .981; n = 6) than native cardiac channels. The differences presumably arise from other residues that differ between the two channels.
23. J. Satin *et al.*, *Science* **256**, 1202 (1992).
24. M. F. Sheets and D. A. Hanck, *J. Physiol.* (*London*), in press.
25. D. T. Yue and E. Marban, *J. Gen. Physiol.* **95**, 911 (1990).
26. We thank G. Breitwieser and G. Yellen for helpful comments on the manuscript and K. Kluge and R. Xu for technical assistance. Supported by the Medical Research Council of Canada (P.H.B.), Established Investigator of the American Heart Association (D.T.Y.), NIH grant K11 HL02639 (J.H.L.), NIH grant RO1 HL36957 (E.M.), and NIH grant K08 HL2421 (G.F.T.).

27 February 1992; accepted 8 May 1992

Block of Ca^{2+} Wave and Ca^{2+} Oscillation by Antibody to the Inositol 1,4,5-Trisphosphate Receptor in Fertilized Hamster Eggs

Shun-ichi Miyazaki,* Michisuke Yuzaki, Ken Nakada, Hideki Shirakawa, Setsuko Nakanishi, Shinji Nakade, Katsuhiko Mikoshiba

The concentration of cytoplasmic free calcium (Ca^{2+}) increases in various stimulated cells in a wave (Ca^{2+} wave) and in periodic transients (Ca^{2+} oscillations). These phenomena are explained by inositol 1,4,5-trisphosphate (IP_3)–induced Ca^{2+} release (IICR) and Ca^{2+}-induced Ca^{2+} release (CICR) from separate intracellular stores, but decisive evidence is lacking. A monoclonal antibody to the IP_3 receptor inhibited both IICR and CICR upon injection of IP_3 and Ca^{2+} into hamster eggs, respectively. The antibody completely blocked sperm-induced Ca^{2+} waves and Ca^{2+} oscillations. The results indicate that Ca^2 release in fertilized hamster eggs is mediated solely by the IP_3 receptor, and Ca^{2+}-sensitized IICR, but not CICR, generates Ca^{2+} waves and Ca^{2+} oscillations.

A dramatic, transient increase in the intracellular calcium (Ca^{2+}) concentration ($[Ca^{2+}]_i$) occurs at fertilization in all eggs investigated so far, observed as a "Ca^{2+} wave" across the egg (*1*). In many species the Ca^{2+} transient is due to release of intracellular Ca^{2+} (*1*) and is required for exocytosis of cortical granules to prevent polyspermy (*1*) and for cell cycle progression (*2*). Fertilized hamster eggs exhibit repetitive Ca^{2+} transients as well as the Ca^{2+} wave in each response (*3*). Ca^{2+} waves and Ca^{2+} oscillations commonly occur in various somatic cells in response to neurotransmitters, hormones, and growth factors (*4*, *5*). These agents stimulate polyphosphoinositide turnover, which leads to IICR (*4*). IICR is suggested to occur in fertilized eggs of the sea urchin (*2*), frog (*6*), and hamster (*7*). On the other hand, IP_3-independent Ca^{2+} release, such as CICR, has also been detected in sea urchin eggs (*8*, *9*) and other cells (*4*). However, it has been difficult to obtain direct evidence for operation of IICR, or of CICR after eliminating IICR, in functioning cells under physiological conditions, because no specific blockers of IICR were available.

IICR and CICR are mediated by the IP_3 receptor (*10*, *11*) and ryanodine receptor (*12*), respectively. The IP_3 receptor has been purified from rat (*10*) and mouse (*11*) cerebella, and its primary structure was determined by cDNA cloning (*13*, *14*). Three monoclonal antibodies (MAbs) to the mouse IP_3 receptor have been obtained (*11*, *13*). The 18A10 MAb, which recognizes an epitope close to the proposed Ca^{2+} channel region in the COOH-terminus of the receptor protein (*13*), inhibits IICR in mouse cerebellar microsomes (*15*), whereas 4C11 and 10A6, which recognize the NH_2-terminal and middle regions, respectively (*13*), block neither IP_3 binding nor Ca^{2+} release in microsomes (*15*). We investigated whether 18A10 could block Ca^{2+} release induced by injection of IP_3 or by sperm in hamster eggs.

In hamster eggs, 18A10 stained the cortical area and inner cytoplasm in a roughly reticular pattern (Fig. 1A) (*11*), consistent with the distribution of smooth endoplasmic reticula (*16*). Eggs were also stained by 4C11 but not by 10A6. We ascertained the specificity of the MAbs by immunostaining of blotted proteins from hamster eggs (Fig. 1B) (*11*). Both 18A10 and 4C11 stained a single 250-kD protein corresponding to the mouse IP_3 receptor (*11*). The 10A6 MAb stained the 250-kD band from eggs faintly, although it reacted strongly with a 250-kD protein from cerebella and ovaries after ovulation of mature eggs. In this report, 4C11 and 10A6 served as controls.

Each MAb was injected into eggs through micropipettes by air pressure, together with the Ca^{2+}-sensitive dye fura 2. Measurement of fluorescence of fura 2 enabled estimation of the injected volume of MAb and measurement of $[Ca^{2+}]_i$ with an image processor (*17*). IP_3 was injected at the margin of the egg 1 to 2 hours later with negative current pulses (Fig. 2), which allowed repeated application of IP_3 in the same egg. The relative amount of IP_3 administered is represented by the magnitude (nA × s) of the square current pulse. The spatial distribution of increases in $[Ca^{2+}]_i$ was analyzed at three areas (Fig. 2).

S-i. Miyazaki, K. Nakada, H. Shirakawa, Department of Physiology, Tokyo Women's Medical College, 8-1 Kawada-cho, Shinjuku-ku, Tokyo 162, Japan.
M. Yuzaki, Department of Biochemistry, Jichi Medical School, Tochigi-ken 329-04, Japan.
S. Nakanishi and S. Nakade, Division of Regulation of Macromolecular Function, Institute for Protein Research, Osaka University, Suita 565, Japan.
K. Mikoshiba, Department of Molecular Neurobiology, Institute of Medical Science, University of Tokyo, Minato-ku, Tokyo 108, Japan.

*To whom correspondence should be addressed.